Theory of transport properties of pure, single crystal zinc

P. G. Tomlinson*
Department of Physics, McMaster University, Hamilton, Ontario L8S 4M1, Canada
and Department of Physics, Indiana University, Bloomington, Indiana 47405
(Received 12 August 1975)

Pseudopotential calculations have been performed by Tomlinson and Swihart to obtain phonon frequencies and polarization vectors, the Fermi surface, band velocities, and multi-orthogonalized-plane-wave electron-phonon matrix elements for pure zinc. These results are then used to determine the electrical and thermal resistivities which result from the scattering of electrons by thermal phonons. The same interaction also contributes to the attenuation of ultrasonic waves and the finite lifetimes of quasiparticle states near the Fermi surface, and these effects are also calculated. The Fermi surface and electron wave functions are based on the extremely accurate fit to de Haas–van Alphen data obtained by Stark and Falicov. Tomlinson and Swihart also make use of their resulting nonlocal pseudopotential for the matrix elements. The phonon model used is based on a pseudopotential calculation, and agrees well with neutron-diffraction data for frequencies at all high-symmetry points and for the polarization vectors where they have been determined. We solve the Boltzmann equation by the variational method, where we assume that the trial distribution function can be well represented as an expansion in up to six spherical harmonics. Solution in terms of different types of trial functions and in terms of anisotropic scattering times are presented for comparison.

I. INTRODUCTION

The pseudopotential theory of metals allows one to calculate many metallic properties within the framework of simple perturbation theory. The theory, as it applies to the electron-phonon interaction, has been worked out by Sham[1] and has been tested by several authors[2-8] on numerical calculations of transport properties and superconductivity. The extent to which such things as realistic phonon models, Fermi surfaces, nonlocality of the pseudopotential, and the multi-OPW (orthogonalized plane wave) nature of the wave functions are important still remains uncertain. The calculations to be described here are of value in answering some aspects of the above questions, as well as in the interpretation of experimental data.

The hexagonal close-packed metal, zinc, was chosen for this study because its structure provides several interesting anisotropic properties, while complications introduced by Fermi-surface distortions, etc., are not so great as to preclude realistic treatment of such. The existence of the extremely accurate pseudopotential fit of Stark and Falicov[9] (SF), which had been used very successfully in previous calculations,[4,5,7] was also a factor in the choice of zinc. Finally, there is a sufficient number of experimental data[10,11] with which to compare our results.

This calculation explores for the first time the effects of realistic band-structure models and higher-order trial functions on the solution of the Boltzmann equation in an hcp metal. Initial results of these calculations have been reported in Ref. 12. Previous calculations in zinc were done by Allen and Cohen[5] for isotropic properties and by Truant and Carbotte for anisotropic properties. Allen and Cohen approximated the Fermi surface by a sphere, the phonon frequencies by an isotropic fit to neutron-diffraction data, single-particle electron states by plane waves (single OPW's), and the phonon Brillouin zone by a Debye sphere. They obtained excellent agreement between their calculated phonon mass-renormalization parameter λ and that extracted from the electronic-specific-heat coefficient and the superconducting transition temperature. Their results for the room-temperature electrical resistivity were low by about 50% and 75% for the SF and Animalu-Heine pseudopotentials, respectively. Truant and Carbotte,[7] using the same assumptions as Allen and Cohen except that they used a force-constant model for the phonons, calculated anisotropic properties as well. Their results for the isotropic mass-enhancement parameter and room-temperature electrical resistivity ρ_{273} were in good agreement with experiment. They explored the sensitivity of their results to different force-constant fits, and found λ and ρ_{273} to be very sensitive to the different fits. Since that calculation, phonon data[13] have become available at many more points in the Brillouin zone, largely removing that uncertainty. Pecheur and Toussaint[8] have calculated the thermal and electrical resistivity under similar assumptions. All but one of the above calculations neglect anisotropy of the electron distribution function, which we find important at low temperature. Truant and Carbotte include this in the form of anisotropic scattering times.

Results of our calculation for Zn (Refs. 12, 14, 15

together with the present paper), that of Nowak[16] for Cu, and recently that of Leung[17] for Al demonstrate that for anisotropic properties one must use more realistic models for the Fermi surface and electron-phonon matrix elements. In this work, the Fermi surface is generated from the Stark-Falicov[9] pseudopotential which was fit to de Haas-van Alphen data. The electron wave functions are based on an expansion in several OPW's (multi-OPW's) also obtained from the SF pseudopotential. The phonon frequencies and polarization vectors are obtained from a pseudopotential model,[15] to whose dynamical matrix,[18] terms resulting from three additional force constants were added. The addition of these force constants was sufficient to cause the calculated frequencies to agree with recent data[13,19] covering all symmetry lines in the Brillouin zone. The details of our calculational model for the phonons, Fermi surface, band velocity, and electron-phonon matrix elements are described in the preceding paper,[14] referred to as I. We employ atomic units, $m_0 = e = \hbar = 1$, throughout.

The theory of transport properties and results are presented in Secs. II and III, respectively, and Sec. IV is set aside for concluding remarks.

II. THEORY

The Kohler variational principle provides a method of solving the Boltzmann equation which is extremely popular due to its great versatility and simplicity of expression. Ziman[20] has demonstrated its use in the treatment of a great many transport problems. It simply states that if an integral equation can be expressed in the form

$$X = P\Phi \,, \tag{1}$$

where X is independent of Φ and P is an integral operator satisfying a few physically nonrestrictive conditions, then of all the functions Φ which obey

$$\langle \Phi, X \rangle = \langle \Phi | P | \Phi \rangle \,, \tag{2}$$

the one that solves Eq. (1) is the one that minimizes the ratio

$$\langle \Phi | P | \Phi \rangle / (\langle \Phi | X | \rangle)^2 \,. \tag{3}$$

The linearized Boltzmann equation can be written in the form of Eq. (1), in which X is the driving force, Φ is the deviation of the distribution function from equilibrium, and P is the scattering operator, in our case arising from the electron-phonon interaction.

If we wish to express the trial function Φ in terms of an expansion in simpler known function ϕ_i,

$$\Phi = \sum_i \eta_i \phi_i \,, \tag{4}$$

then the η_i which minimize expression (3) also minimize the resistivity which is then

$$\rho = \left(\sum_{ij} X_i (P^{-1})_{ij} X_j \right)^{-1} , \tag{5}$$

where

$$X_i = \langle \Phi_i | X \rangle \tag{6}$$

and

$$P_{ij} = \langle \Phi_i | P | \phi_j \rangle \,. \tag{7}$$

A. Electrical resistivity

The distribution function $f_{\vec{k}}$ in the presence of a uniform electric field of unit strength $\vec{u}$ may be expressed as

$$f_{\vec{k}} = f^0_{\vec{k}} - \Phi(k) \frac{\partial f^0_{\vec{k}}}{\partial E_{\vec{k}}} \,, \tag{8}$$

where $f^0_{\vec{k}}$ is the equilibrium distribution function and contributes nothing to the current. Keeping only terms that are linear in $\vec{u}$, we obtain

$$\vec{v}_{\vec{k}} \cdot \vec{u} \, \frac{\partial f^0_{\vec{k}}}{\partial E} = \frac{1}{k_B T} \sum_{\vec{k}'} (\Phi_{\vec{k}'} - \Phi_{\vec{k}}) P^{\vec{k}'}_{\vec{k}} \,, \tag{9}$$

where k_B is the Boltzmann constant and $P^{\vec{k}'}_{\vec{k}}$ is the net equilibrium probability of scattering from state $\vec{k}$ to $\vec{k}'$. Equation (9) is in the form of Eq. (1), and thus the resistivity is given by Eq. (5) with

$$X_i = \frac{1}{4\pi^3} (\tfrac{1}{3} 4\pi)^{1/2} \int_{FS} d^2k \, Y_{10}(\theta, \Phi) \Phi^*_i(\theta, \Phi) \,, \tag{10}$$

where θ and ϕ are polar coordinates such that the direction of the applied field determines the polar axis and $Y_{10}(\theta, \phi)$ is a spherical harmonic. The P_{ij} are given by

$$P_{ij} = \frac{2\beta k_F}{\pi} m^*_b \int_0^\infty \alpha^2_{ij} F(\omega) \frac{\omega \, d\omega}{(1 - e^{-\beta\omega})(e^{\beta\omega} - 1)} \,, \tag{11}$$

where $\beta = 1/k_B T$ and m^*_b is the band mass. The function $\alpha^2_{ij} F(\omega)$ is given by

$$\alpha^2_{ij} F(\omega) = \left((2\pi)^3 \int_{FS} \frac{d^2k}{v_{\vec{k}}} \right)^{-1} \int_{FS} \frac{d^2k'}{v_{\vec{k}'}} \int_{FS} \frac{d^2k}{v_{\vec{k}}} [\phi_i(\vec{k}') - \phi_i(\vec{k})][\phi_j(\vec{k}') - \phi_j(\vec{k})] \sum_\lambda |g_{\vec{k}\vec{k}'\lambda}|^2 \delta(\omega - \omega_{\vec{q}\lambda}) \,. \tag{12}$$

In the above $g_{\vec{k}\vec{k}'\lambda}$ is the electron-phonon matrix element for scattering from state $\vec{k}$ to $\vec{k}'$ via a phonon of reduced wave vector q, mode λ, and frequency $\omega_{\vec{q}\lambda}$. Also, $v_{\vec{k}}$ is the band velocity. We have assumed that the phonons remain in their equilibrium state, thus neglecting phonon drag effects. For a pseudo wave function expanded in terms of plane waves $|\vec{k}\rangle$,

$$\phi_{\vec{k}} = \sum_{\vec{G}} a_{\vec{G}}(\vec{k})\,|\vec{k}+\vec{G}\rangle\,, \tag{13}$$

where $\vec{G}$ is a reciprocal-lattice vector, the matrix element is given by

$$g_{\vec{k}'\vec{k}\lambda} = \frac{i(i-1)}{\sqrt{2}}\left(\frac{1}{2NM\omega_{\vec{q}\lambda}}\right)^{1/2}\sum_{\vec{G}'\vec{G}}[a_{\vec{G}'}(\vec{k}')]^* a_{\vec{G}}(\vec{k})\,w(\vec{k}+\vec{G},\vec{Q})\vec{Q}$$
$$\times\tfrac{1}{2}\{\vec{f}^{\lambda}(\vec{q},1)[\cos(\vec{Q}_0\cdot\vec{\rho})-\sin(\vec{Q}_0\cdot\vec{\rho})]+\vec{f}^{\lambda}(\vec{q},2)[\cos(\vec{Q}_0\cdot\vec{\rho})+\sin(\vec{Q}_0\cdot\vec{\rho})]\}\,. \tag{14}$$

In the above $\vec{Q}=\vec{k}'+\vec{G}'-(\vec{k}+\vec{G})$, and $\vec{q}$ is a vector in the first Brillouin zone such that $\vec{k}'-\vec{k}+\vec{G}'-\vec{G}=\vec{Q}_0+\vec{q}$ and $\vec{Q}_0$ is a reciprocal-lattice vector. $w(\vec{k},\vec{q})$ is the nonlocal pseudopotential form factor, N is the number of atoms, and M is the atomic mass. The position vector $\vec{\rho}$ and the polarization vectors $\vec{f}^{\lambda}(q,M)$ are described in I. Thus the problem of electrical resistivity is reduced to that of choosing an appropriate trial function and performing the numerical integrations of Eqs. (10) and (12).

The Fermi surface of Stark and Falicov differs from a spherical model in that the so-called butterflies and stars are absent. These sections of Fermi surface have never been observed experimentally. The expansion coefficients $a_{\vec{G}}(\vec{k})$ are determined simultaneously with the Fermi surface, as is discussed in I. In Eq. (12) $v_{\vec{k}}$ is the band Fermi velocity, and is obtained by numerically differentiating the band energy as discussed in I. As we note there, a different energy dependence must be incorporated in the SF pseudopotential in determining the band velocity. We do this by scaling[21] the integrals by the ratio 0.61/0.54.

The pseudopotential form factor in the electron-phonon matrix element Eq. (14) is also a version of the SF pseudopotential. However, this pseudopotential is determined only at reciprocal-lattice vectors, so an interpolation through the fitted points as well as an extrapolation to $q=0$ is required. We determine the local part of the pseudopotential by taking a spline interpolation through the SF points at large q and contouring the small and intermediate q portion, so that for k and k' on a spherical Fermi surface the total form factor is identical to Shaw's optimized model potential.[22] After some preliminary calculations with the version screened in the Hartree approximation, it was apparent that our results were too low (about 30% for λ). We found that by incorporating Shaw's theory of k-dependent effective masses[23] into his pseudopotential, the long-wavelength limit was considerably increased in magnitude and good agreement was achieved with a great deal of experimental evidence as reported in Refs. 12, 14, and 15. Later we became aware of the work of Appapillai and Williams,[24] in which they applied corrections due to exchange and correlation and a more satisfactory treatment of the k-dependent mass correction. The effect also increased the magnitude of the pseudopotential near $q=k_F$, and where the quasiparticle lifetimes and electrical resistivity were recalculated with this form factor the results were only about 5% lower than those previously obtained. For this reason the calculations for the thermal resistivity and the ultrasonic attenuation were not repeated.

At this point we should emphasize that we are not arbitrarily piecing together different form factors, but looking for a suitable extrapolation of SF to small and intermediate values of q. We feel that if we are guided by experimental data we may learn something about the nature of the physics involved. As it turns out, the pseudopotential derived by Moriarty,[25] after our calculations were completed, very closely resembles our combination SF and Appapallia and Williams pseudopotential. It would presumably generate a realistic Fermi surface and give reasonable Fermi velocities. Since Moriarty's pseudopotential is based on firm theoretical ground and also does a good job in predicting the correct phonon frequencies and c/a ratio in zinc, we are confident that our form factor is among the best available.

For the case of electrical resistivity the trial basis functions were chosen equal to spherical harmonics times the Fermi band velocity

$$\phi_i(\vec{k}) = v_{\vec{k}}\,Y_{LM}(\theta,\phi)\,. \tag{15}$$

Only those $Y_{LM}(\theta,\phi)$ which have the symmetry of

an hcp metal in an electric field are allowed. That is, for $\vec{u}$ in the c direction

$$L = 1,\ 3,\ 5,\ \ldots$$

$$M = 0,\ 6,\ 12,\ \ldots\ .$$

Out of this set we were limited by practical considerations to six. We were guided by the variational principle to those functions that yielded the set of X_i with maximum values. Thus the choice was made essentially on the basis of the Fermi-surface geometry. Subsequently, the ϕ_i from this smaller set are used to minimize the resistivity as in Eq. (5).

For the case of $\vec{u}$ parallel to the c axis we obtain

$$Y_{1,0};\quad Y_{3,0};\quad Y_{7,0};\quad Y_{7,6};\quad Y_{9,0};\quad Y_{9,6}.$$

Throughout this paper we use the real definition of spherical harmonics in which $e^{im\phi}$, in the usual definition, is replaced by $\sqrt{2}\cos\phi$. For $\vec{u}$ along the $\langle 11\bar{2}0\rangle$ direction we retain the c axis as the polar axis, because the symmetry of the Fermi surface is easily obtained in these coordinates. We expand the trial function in terms of $v_{\vec{k}}$ times the following functions:

$$Y_{11};\ Y_{5,1};\quad Y_{7,1};\quad (Y_{5,5}+Y_{5,7});\quad Y_{9,1};$$
$$(Y_{13,11}+Y_{13,13}).$$

We have also calculated the electrical resistivity for the case of the trial function

$$\phi_i(\vec{k}) = v_{\vec{k}}\cos\theta(v_{\vec{k}}/\langle v_{\vec{k}}\rangle)^{40(i-1)} \tag{16}$$

where θ is measured from u and $\langle v_k\rangle$ is the Fermi-surface average of $v_{\vec{k}}$. For future reference we shall label the spherical harmonic expansion as trial function A and the latter as trial function B. This latter trial function was suggested by the work of Bergman, Kaveh, and Wiser,[26] but as we shall see the solution in terms of spherical harmonics is slightly better for Zn. That is, the resulting resistivities are lower. A third solution in terms of the usual trial function

$$\Phi(k) = v_{\vec{k}}\cos(\theta), \tag{17}$$

where θ is the angle between $\vec{k}$ and $\hat{u}$, is obtained for comparison.

Another way of solving the Boltzmann equation is by the use of anisotropic scattering times defined by

$$\frac{1}{\tau_i(\vec{k},T)} = 4\pi\beta\int_0^\infty \frac{d\omega\,\omega}{(1-e^{-\beta\omega})(e^{\beta\omega}-1)}\left(\frac{1}{2}\pi\right)^3\int_{FS}\frac{d^2k'}{v_{\vec{k}'}}\left(1-\frac{\tau_i(\vec{k}',T)}{\tau_i(\vec{k},t)}\,\frac{v_i(\vec{k}')}{v_i(\vec{k})}\right)\sum_\lambda |g_{\vec{k}'\vec{k}\lambda}|^2\delta(\omega-\omega_{\vec{q}\lambda}), \tag{18}$$

where $v_i(\vec{k})$ is a Cartesian component of the band Fermi velocity $\vec{v}(\vec{k})$. The resistivity is then given by

$$\rho(T) = \left(\frac{1}{12\pi^3}\int_{FS}\frac{d^2k}{v_{\vec{k}}}[v_i(\vec{k})]^2\tau_i(k,T)\right)^{-1}. \tag{19}$$

In principle Eq. (18) could be iterated to convergence at each value of T, but it is impractical to do so. Instead, we make the right-hand side of Eq. (18) independent of $\tau_i(\vec{k},T)$ by initially assuming them to be independent of $\vec{k}$. Sorbello[27] has found this approximation to be unsatisfactory for the case of residual resistivity due to substitutional impurities. However, the values we obtain for the resistivity are equal to those obtained by the variational principle to within numerical accuracy. In practice, the Fermi-surface integral in Eq. (18) was performed at 37 points on the Fermi surface.

The scattering times were then calculated at various temperatures, interpolated, and then used in Eq. (19). These results are presented in Table I.

B. Thermal resistivity

For a conductor in a thermal gradient in the absence of electric fields the Boltzmann equation is given by

$$\vec{v}_{\vec{k}}\cdot\vec{\nabla}T\,\frac{\partial f_{\vec{k}}}{\partial T} = \dot{f}_k\Big|_{scatt}. \tag{20}$$

Following the usual procedure, we take the trial function to be linear in energy, i.e., of the form of Eqs. (8) and (4) with

$$\phi_i(\vec{k}) = (E_{\vec{k}} - E_F)Y_{LM}(\theta,\phi). \tag{21}$$

Again Eq. (5) gives us the resistivity, but the P_{ij} are now defined as

$$P_{ij}^{th} = \frac{1}{L_0T}\,\frac{2\beta k_F}{\pi}\,m_b^*\int_0^\infty\frac{\omega\,d\omega}{(1-e^{-z})(e^z-1)}\left[\alpha_{ij}^2F(\omega)\left(1+\frac{Z^2}{\pi^2}\right)+\frac{3}{\pi^2}\,\alpha_{ij}^{-2}F(\omega)Z^2\right], \tag{22}$$

where $Z=\beta\omega$ and $L_0=\frac{1}{3}\pi^2k_B^2$, the Lorentz number. The function $\alpha_{ij}^2F(\omega)$ is given by

$$\alpha_{ij}^2F(\omega)=\frac{(1/2\pi)^3\int_{FS}(d^2k/v_{\vec{k}})\int_{FS}(d^2k'/v_{\vec{k}'})[\phi_i(\vec{k})\phi_j(\vec{k}')]\sum_\lambda|g_{\vec{k}\vec{k}'\lambda}|^2\delta(\omega-\omega_{\vec{q}\lambda})}{\int_{FS}(d^2k/v_{\vec{k}})}\ , \tag{23}$$

and is calculated simultaneously with the $\alpha_{ij}^2F(\omega)$. The derivation of Eq. (22) follows that of Ziman[20] (p. 388). We simply retain the more general trial function.

This calculation was performed with a different choice of spherical harmonics and the form factor given by the solid curve of Fig. 1. The electrical resistivity has also been calculated under these assumptions, and is presented elsewhere.[12] The spherical harmonics used in the thermal resistivity are

$$Y_{1m},\ Y_{3m},\ Y_{5m},\ Y_{7m},\ Y_{9m},\ \text{and}\ Y_{15m},$$

with $m=0,1$ for $\vec{\nabla}T$ parallel and perpendicular to the c axis, respectively.

C. Ultrasonic attenuation

Scattering times appropriate to the attenuation of ultrasonic waves were calculated in the limit of $q v\tau \ll 1$ following Steinberg,[28] where v is the Fermi velocity.

Steinberg shows that for a wave traveling along the ith coordinate with a velocity gradient β along the jth coordinate, the Boltzmann equation is

$$-\beta v_i(\vec{k})v_j(\vec{k})\frac{\partial f_k^0}{\partial E}=\dot{f}_{\vec{k}}\Big|_{\text{scatt}}\ . \tag{24}$$

We take the distribution function to be of the form

$$f_{\vec{k}}=f_{\vec{k}}^0+\beta\tau_{2m}v_i(\vec{k})v_j(\vec{k})\frac{\partial f_{\vec{k}}^0}{\partial E}\ . \tag{25}$$

We define τ_{2m} ($m=0$ for dilatational waves and $m=1$ for shear waves) such that

$$(f_{\vec{k}}-f_{\vec{k}}^0)/\tau_{2m}=\dot{f}_{\vec{k}}|_{\text{scatt}}\ . \tag{26}$$

This gives, assuming the $v(\vec{k})$ are isotropic,

TABLE I. Numerical results for electrical and thermal resistivity. Results for electrical resistivity are for trial function A in units of Ω cm. For thermal resistivity units are cm K/W. The superscript 0 indicates the directional trial function was replaced by the simple $v_k\cos(\theta)$. Values for η_i [Eq. (4)] are those that minimize $\rho_\parallel$. ρ^{ST} is the scattering-time resistivity.

T (K)	7	10	20	40	50
$\rho_\parallel$	0.75×10^{-10}	0.14×10^{-8}	0.55×10^{-7}	0.38×10^{-6}	0.58×10^{-6}
$\rho_\perp$	0.33×10^{-9}	0.23×10^{-8}	0.45×10^{-7}	0.32×10^{-6}	0.52×10^{-6}
$\rho_\parallel/\rho_\perp$	0.23	0.61	1.22	1.17	1.12
$w_\parallel$	8.5	27.0	290	660	750
$w_\perp$	10.9	50.5	315	705	790
$w_\parallel/w_\perp$	0.78	0.535	0.923	0.935	0.95
$\rho_\parallel/\rho_\parallel^0$	0.48	0.88	0.92	0.915	0.92
$\rho_\perp/\rho_\perp^0$	0.48	0.82	0.97	0.98	0.98
$w_\parallel/w_\parallel^0$	0.59	0.92	0.97	0.99	0.99
$w_\perp/w_\perp^0$	0.81	0.93	0.96	0.98	0.98
$\rho_\parallel{}^{ST}$	0.85×10^{-10}	0.17×10^{-8}	0.58×10^{-7}	0.38×10^{-6}	0.60×10^{-6}
$\rho_\perp{}^{ST}$	0.98×10^{-9}	0.25×10^{-8}	0.45×10^{-7}	0.33×10^{-6}	0.54×10^{-6}
η_2/η_1	2.52	0.785	−0.392	−0.450	−0.436
η_3/η_1	1.18	0.454	0.193	0.162	0.153
η_4/η_1	1.15	0.396	−0.075	−0.156	−0.166
η_5/η_1	−0.40	−0.248	−0.127	−0.130	−0.127
η_6/η_1	−0.03	0.138	0.081	0.058	0.056

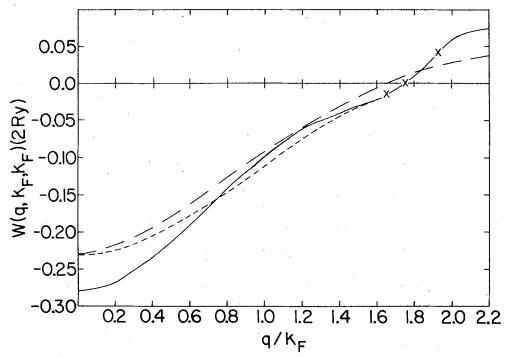

FIG. 1. On-the-Fermi-surface form factor. The ×'s are the fitted points of Stark and Falicov (Ref. 9). The long-wavelength portion is contoured to agree with that of Shaw (Refs. 22 and 23), solid curve; and Appapillai and Williams (Ref. 24), short-dashed curve. The long-dashed curve is the Hartree version of Shaw's potential with $m^*=1$.

$$\frac{1}{\tau_{20}} = 64\pi^4 \langle Y_{20}|P|Y_{20}\rangle \Big/ \left(45 \int_{FS} \frac{d^2k}{v_k} \cos^4(\theta)\right)$$
$$\frac{1}{\tau_{21}} = 4\pi^3 \langle Y_{21}|P|Y_{21}\rangle \Big/ \left(\int_{FS} \frac{d^2k}{v_k} |Y_{21}(\theta,\phi)|^2\right), \quad (27)$$

where the numerators are defined by Eqs. (7) and (11). Once the scattering times are calculated, the attenuation coefficients are given by Bhatia and Moore.[29]

It is difficult to compare with experimental data[30] in the limit $qv\tau \ll 1$, because at higher temperatures, where τ is small, phonon-phonon processes dominate electron-phonon processes. The ultrasonic attenuation is of theoretical interest, however, in examining the effect of the different types of distribution function on the temperature dependence of the scattering time. We find, for instance, that at high temperatures the ultrasonic attenuation is much more sensitive to different crystal orientations than the electrical or thermal resistivity. The pseudopotential form factor used was the solid curve of Fig. 1. The expressions for the ultrasonic-attenuation scattering times that appear here are different from those of Ref. 12. In Ref. 12 we took the distribution function to be proportional to $Y_{2m}(\theta,\phi)$, which is not the best choice in the case of $m=0$. We also failed to correct for the normalization factors of the Y_{2m}'s. The current expressions are correct and the ones of Ref. 12 may be disregarded.

D. Quasiparticle lifetimes

Though not itself generally considered a part of transport theory, the lifetime of a quasiparticle at the Fermi surface is often thought of in connection with transport scattering times. The latter are not lifetimes at all since they, in effect, measure not only the probability of an electron being scattered, but the effect of such scattering in damping the flow of current or heat, for instance. Measurements that are thought to probe quasiparticle lifetimes are amplitude signals of cyclotron resonance,[32] radio-frequency size effect,[31] and magnetic-surface-states[33] experiments.

To calculate quasiparticle lifetimes we do not have to solve a Boltzmann equation. Instead, we know that the lifetime is related to the imaginary part of the electron self-energy $\Sigma(k,\omega)$. Considering only effects due to scattering from thermal phonons, we have

$$[\tau_{\text{el-ph}}(\vec{k},\omega)]^{-1} = 2\,\text{Im}\Sigma_{\text{ph}}(\vec{k},\omega). \quad (28)$$

By appealing to Migdal's theorem, this expression can be made tractable, and at the Fermi surface ($\omega=0$) we have

$$\frac{1}{\tau_{\text{el-ph}}(\vec{k})} = 4\pi \int d\omega'\, \alpha^2F(\vec{k},\omega')\left(\frac{1}{e^{\beta\omega'}+1} + \frac{1}{e^{\beta\omega'}-1}\right). \quad (29)$$

The expression $\alpha^2F(\vec{k},\omega)$ is well known from the theory of superconductivity, and is easily calculated along with transport properties:

$$\alpha^2F(\vec{k},\omega) = \frac{1}{(2\pi)^3} \int \frac{d^2k'}{v_{\vec{k}'}} \sum_\lambda |g_{\vec{k},\vec{k}'\lambda}|^2 \delta(\omega - \omega_{\vec{q}\lambda}). \quad (30)$$

The pseudopotential used in calculating $\tau_{\text{el-ph}}(\vec{k})$ is the combination of SF and Appapallia and Williams (short-dashed curve of Fig. 1). Results using the other pseudopotential (solid curve of Fig. 1) have been presented elsewhere.[12]

III. RESULTS

A. Electrical resistivity

In Fig. 2 we plot the calculated temperature dependence of $\rho_\parallel$ ($\hat{u}$ parallel to the c axis) and $\rho_\perp$ ($\hat{u}$ perpendicular to the c axis) for trial function A, along with experimental data.[10] The comparison is quite good at all temperatures. Although we are off by approximately a factor of 2 at $T \ll 14$°K, this does not indicate that there is anything seriously wrong with the calculation. Small errors in the phonon spectrum could greatly affect the results at this temperature. At low temperatures phonon-drag effects become important, also. Furthermore, at very low temperatures the experimental accuracy goes down, since the resistivity is dominated by impurity scattering.

At low temperatures we see that $\rho_\parallel \propto T^{3.1}$ and $\rho_\perp$

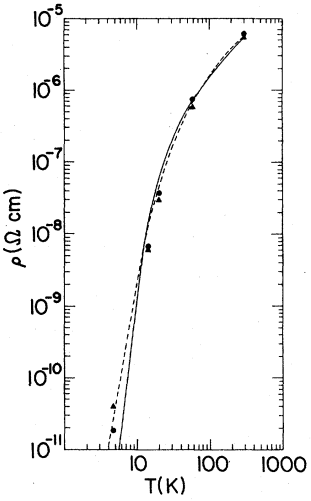

FIG. 2. Temperature dependence of the electrical resistivity. $\rho_{\parallel}$ and $\rho_{\perp}$ are shown by the solid and dashed curves, respectively. Experimental data of Ref. 10 is shown by ● ($\rho_{\parallel}$) and ▲ ($\rho_{\perp}$).

$\propto T^{5.7}$. Deviations from the T^5 law are usually associated with the effect of umklapp processes, but ours stem mainly from the temperature dependence of the distribution function. Using the $v_{\vec{k}}\cos\theta$ trial function, we get $\rho \propto T^{4.8}$. In Fig. 3 we explore the effect of the temperature dependence of the distribution function by plotting the ratio of ρ/ρ_0, where ρ_0 is obtained by using only the first term in the trial function expansion. That is, $\phi_1 = v_{\vec{k}}\cos\theta$, which in the past has been used extensively. We see that this trial function is quite good at higher temperatures and quite poor at low temperatures. There is a peak in the curve at approximately 12 °K which must be explained in terms of competition between two types of processes, each trying to affect the trial function in different ways. These are

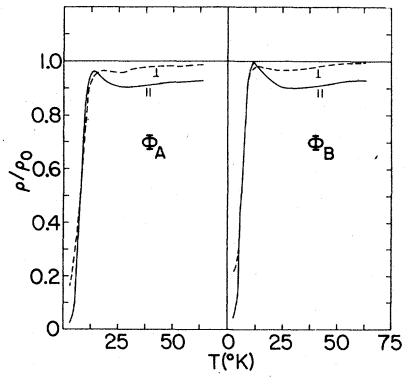

FIG. 3. Ratio of the resistivity $\rho(T)$ to that obtained by the simple trial function $|\vec{v}_{\vec{k}}|\cos\theta$, $\rho^0(T)$. Results are shown using both trial function A and B.

the extremely low-frequency umklapp processes, which can only occur at points near Bragg planes, and the much more numerous but higher-frequency transverse phonon processes which arise from scattering where $\vec{k}' - \vec{k}$ is parallel to the c axis. The importance of the latter is clearly shown in the first large peak in $\alpha^2_{11}F(\omega)$ plotted in Fig. 4. As the temperature is lowered below 10 °K, the latter are given much less weight from the thermal factors in Eq. (11), and the resistivity is dominated by scattering from relatively isolated regions of the Fermi surface near Bragg planes. Thus it is simpler to find a distribution function that will significantly lower the resistivity by giving these regions less weight.

The similarity of the curves in Fig. 3 arising from trial function A and B demonstrates that we probably will not be able to lower the resistivity much by trying other types of trial functions. Unfortunately, this also demonstrates that the resistivity is not sensitive to the details of the distribution function and, at least in this case, we cannot determine physically important distribution functions (important, for example, for deviations from Matthiessen's rule and the Hall effect) from the variational principle.

Also plotted (Fig. 5) is the ratio $\rho_{\parallel}/\rho_{\perp}$ using trial function A. Experimental data are also plotted and good qualitative agreement is obtained at all temperatures.[41] We do not attach much importance to the fact that in contradiction to experimental data we get $\rho_{\parallel}/\rho_{\perp} < 1$ for high temperature, because both theory and experiment give a ratio close to unity. Small changes in the phonon spectrum and correction for multiphonon processes could reverse the ratio quite easily.

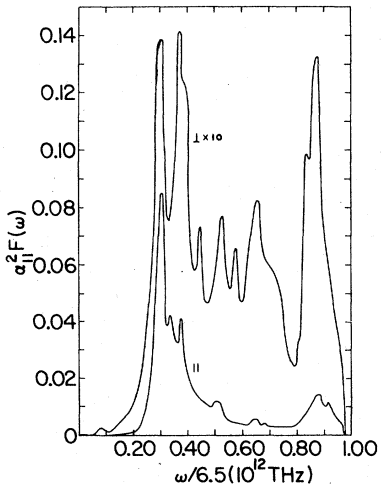

FIG. 4. Functions $\alpha^2_{11}F(\omega)$ for $\vec{u}\|\vec{c}$ (lower curve) and $\vec{u}\perp\vec{c}$ (upper curve). The upper curve has been multiplied by a factor of 10 for clarity.

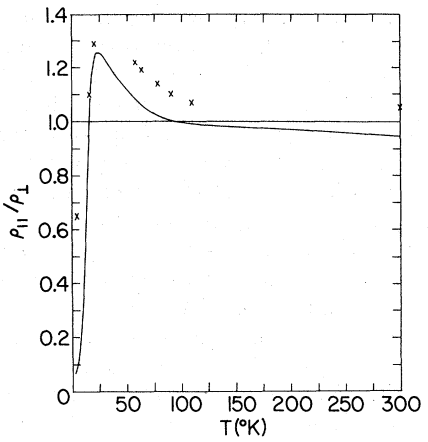

FIG. 5. Ratio $\rho_{\parallel}/\rho_{\perp}$ is plotted as a function of temperature. The solid line is from the calculation and the ×'s are the experimental data of Ref. 10.

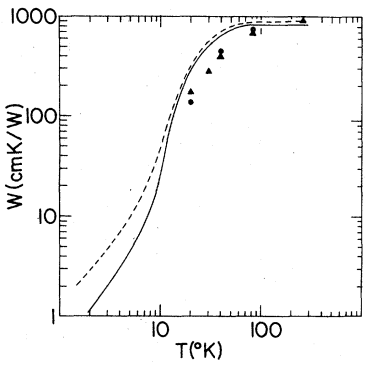

FIG. 6. Thermal resistivity as a function of temperature. $w_{\parallel}$ and $w_{\perp}$ are plotted as the solid and dashed curves, respectively. The experimental data are from Ref. 11 and are represented by ● ($w_{\parallel}$) and ▲ ($w_{\perp}$). The point at 273 °K is taken from Ref. 40.

It is remarkable that the high-temperature resistivity is so isotropic for zinc, since the X_i's and P_{ij}'s separately are quite anisotropic, as one can conclude from Fig. 4. If the scattering term P_{11} were isotropic, as might be the case for the residual resistivity, the Fermi-surface geometry alone, as reflected in X_1, would cause an anisotropy of $\rho_{\perp} \simeq 2.7\rho_{\parallel}$.

In Table I we list resistivities obtained by the scattering time formula of Eqs. (18) and (19). Judging from the close agreement between these results and those obtained by assuming totally different forms of trial functions in the variational formulas, we conclude that our solution to the Boltzmann equation is very nearly exact. The discrepancy at lower temperatures is probably due to the fact that the scattering time is too anisotropic for accurate interpolation of $\tau(\vec{k})$ between the points at which it is calculated.

B. Thermal resistivity

In Fig. 6 we plot the thermal resistivity as a function of temperature. The agreement with experimental data[11] is not quite as good as we had with the electrical resistivity. It is thought that the theoretical resistivity can be lowered by as much as 30% by putting a better energy dependence into the trial function of Eq. (21), and there is no doubt that agreement with experiment could be improved by doing so. In this work, however, we are more interested in examining the importance of anisotropy of the distribution function. We find that $\rho^{\text{th}}/\rho_0^{\text{th}}$, the ratio of the resistivity obtained with the higher-order trial function to that obtained by retaining only the first term, is closer to unity even at low temperatures, as was the case for electrical resistivity (Table I). This is due to the fact that at low temperatures the thermal resistivity is dominated by the change in energy rather than the change in direction of the electrons, and the former is more isotropic.

Returning to Fig. 6, we note that the experimental values of $\rho_{\perp}$ and $\rho_{\parallel}$ cross at around 30°K, whereas the theoretical curves do not. Pecheur and Toussaint[8] found that in their calculation the curves did indeed cross. They included no band-structure effects, and used a phonon model different from ours. They ascribed the crossing as due to an inelastic term peculiar to anisotropic metals. However, we include the same inelastic term and do not get the crossing. As in the case with electrical resistivity, it is at high temperatures that our ratio is wrong, and the error could be accounted for by the neglect of multiphonon processes and small changes in the phonon spectrum. In any case, both theory and experiment give almost isotropic results at high temperatures.

C. Ultrasonic attenuation

We repeat that comparison with experiment is difficult for the ultrasonic attenuation because of our restrictive assumption that $qv\tau \ll 1$. We note from Fig. 7 that the attenuation is much more anisotropic than the electrical or thermal resistivity at high temperatures. This is probably due to the Fermi-surface geometry. Lea, Llewellyn, Peck, and Dobbs[30] found that the impurity limited attenuation of longitudinal waves in zinc was anisotropic by a factor of 20, and the ordering is the same as our curves 1 and 2. At low temperatures the power law for the calculated longitudinal waves propagating along the c axis is $\tau_2 \propto T^{-5.1}$.

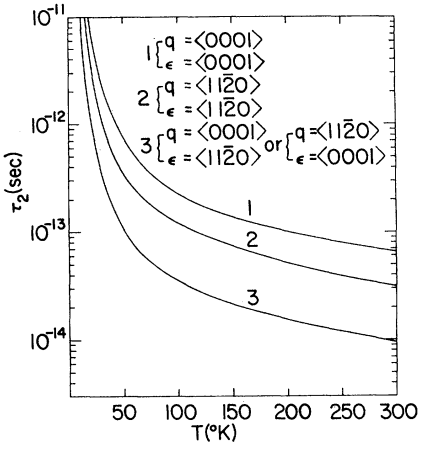

FIG. 7. Scattering times appropriate to ultrasonic attenuation as a function of temperature.

D. Quasiparticle lifetimes

Since quasiparticle lifetimes can be measured at specific points on the Fermi surface by the study of magnetic surface states,[33] we plot our results as a function of Fermi-surface position (Fig. 8). One can also determine orbital averages for lifetimes from the analysis of Azbel-Kanér cyclotron resonance[32] and size-effect data.[31] We note that there are essentially two sources of anisotropy: one slowly varying due to anisotropies in the phonon spectrum, and one rapidly varying due to band-structure effects. The latter seem to occur only as one nears Bragg planes and are due to the multi-OPW nature of the electronic wave functions. We also note that as the temperature increases, most of the phonon-induced anisotropy goes away, but that that due to band structure remains.

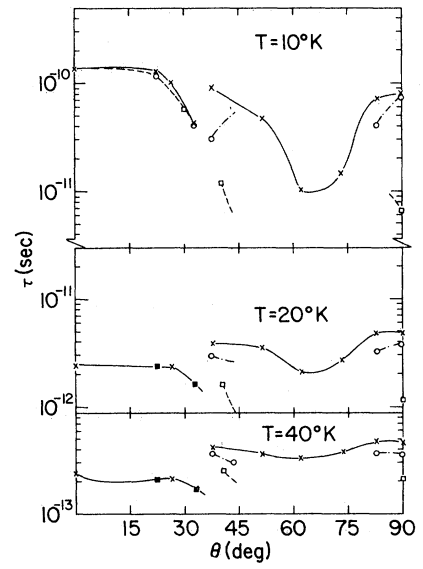

FIG. 8. Quasiparticle lifetimes due to phonons as a function of Fermi-surface position are plotted at various temperatures. θ is the polar angle measured from the c axis. Results are plotted for three azimuthal angles ϕ (measured from $\langle 11\bar{2}0\rangle$: —— ×, $\phi = 0$; —— —— ○, $\phi = 15°$, and — — — — □ for $\phi = 30°$.

It is generally accepted that $[\tau_{\text{el-ph}}(\theta, \phi)]^{-1}$ goes as T^3 at low temperatures, and this is based on a Debye spectrum with frequency-independent electron-phonon parameter. We note that this is probably a reasonable approximation for the Fermi-surface averaged $\langle \tau^{-1}_{\text{el-ph}} \rangle_{\text{FS}}$ but not for each point separately. For instance, between 10 and 20°K, $\tau_{\text{el-ph}}(0,0)$ decreases by a factor of 54, while $\tau_{\text{el-ph}}(61,0)$ only decreases by a factor of 5. Between 5 and 15°K a T^4 dependence is probably more correct even for the Fermi-surface average. However, one should point out that the low-frequency peak due to transverse phonons contributes a significant amount even at 10°K, so that in comparing with accepted power laws one should realize that the assumption of a Debye spectrum is not valid except at very low temperatures. Below 6°K, a $T^{3.5}$ law holds quite well for $\langle \tau^{-1}_{\text{el-ph}} \rangle$. In comparing with experimental data, one should note that we have determined lifetimes only at the Fermi surface. Experimentally one measures a mean lifetime of electrons in a thermal layer of states near the Fermi surface. Allen[34] has determined that in the limit as $T \to 0$ the apparent inverse lifetimes are given by Eq. (29) multiplied by a factor of $\frac{12}{7}$.

There are two recent experiments in which the quasiparticle lifetimes in zinc have been measured. Brookbanks,[35] using cyclotron resonance, measured a lifetime for the central orbit of the lens which goes as T^{-3} for temperatures below 4.2°K. Myers, Thompson, and Ali,[36] using the radio-frequency size effect found that on the lens their inverse scattering lengths λ^{-1}_{th} go approximately as $T^{4.6}$ and on the monster nearly as T^3. The latter authors note that a single scattering will not necessarily remove an electron from the signal. They also note that if the angle of scattering required to remove an electron is large enough, a T^5 law will hold for λ^{-1} and that this may be a possible explanation for the discrepancy between their results and those of Brookbanks.

As far as power laws are concerned, out data are consistent with those of both experiments. We note that Myers *et al.* sample a larger temperature range and that the convincing data occur for $4 \leq T \leq 7$°K. In Table II we report our results along with experimental data. For theoretical λ^{-1}_{th} we divide the inverse lifetimes by phonon renormalized Fermi velocities and scale by $\frac{12}{7}$ as discussed above. We note that for points on the lens a pure power

TABLE II. Comparison of theoretical and experimental scattering lengths. Theoretical values are taken from representative points—not orbital averages. The parameter α is defined such that $\lambda^{-1} = AT^{\alpha}$.

Location on Fermi surface	λ^{-1} (mm^{-1}) Theor.	Expt.	α Theor.	Expt.
Central lens orbit	0.21	1.0 [b]	5.6 [c]	4.6 [b]
		0.43 [a]	2.9 [d]	3.0 [a]
Lens rim orbit	1.08	0.40 [b]	4.7 [c]	4.6 [b]
			2.7 [d]	
Limit point on the monster arms	1.49	1.3 [b]	3.1 [e]	2.9 [b]

[a] Reference 35.
[b] Reference 36.
[c] $T \geq 5$ °K.
[d] $T \leq 4$ °K.
[e] $T \leq 10$ °K.

law is not observed in the calculation. Instead, below 4°K we obtain roughly a T^3 behavior, and above 5°K we see an approximate T^5 dependence. Unfortunately, below 10°K our calculation is subject to rather large statistical errors. We employ a Monte Carlo technique (see I), and out of all possible scattering relatively few are possible at low temperatures. We also note that with such strong temperature dependence our results at any given temperature are strongly dependent on the exact details of the phonon spectrum for small $|q|$. Our treatment of the phonons at small $|q|$ (see I) is crude and was not designed for accurate calculations of lifetimes at very low temperatures. Also, at these temperatures the assumption that the pseudopotential is adequately described in free-electron theory does not hold. In fact, the long-wavelength limit should be inversely proportional to the density of states at the Fermi energy. This would increase $w(\vec{k}, \vec{q})$ by a factor of 1.64 for $|q| \lesssim 0.1|k_F|$, which would increase the contribution of normal processes to $\tau^{-1}_{\text{el-ph}}$ ($T \leq 10$°K) by a factor of 2.7. Thus, though this part of our calculation is crude, we still conclude that the T^{-3} law is by no means sacred and that our results are consistent with experimental data.

IV. DISCUSSION

By calculating in detail the contribution of the electron-phonon interaction to the several transport and other properties of zinc, we have demonstrated that the theory based on pseudopotentials is essentially correct. By realistically treating the Fermi surface and electron wave functions by multiple OPW's, we have achieved good agreement with a great deal of experimental data. In addition, we have demonstrated that the band structure introduces additional anisotropies which should be observed in, for instance, a study of magnetic surface states.[33]

In the process of choosing a suitable pseudopotential for use in the calculation, it becomes clear that beyond a certain point, the effects of nonlocality and exchange and correlation cannot be ignored. A certain amount of nonlocality was required by SF to fit the Fermi surface. We, as well as Auluck,[37] later found that their empirical form was insufficient to calculate Fermi velocities which involve derivatives of the form factor with respect to $\vec{k}$. In extrapolating to small and intermediate values of q we were guided by the optimized model potential of Shaw. Here we found that only when exchange and correlation effects are included is good agreement with transport data achieved (this, of course, depends on which phonon model one uses, but ours is in much better agreement with neutron-diffraction data than are the others which are available). At the time of this calculation there was no single pseudopotential form factor for zinc that would be adequate for generating the Fermi surface, band velocities, matrix elements, and phonons. It would have to be dependent upon $\vec{k}$ and $E_{\vec{k}}$ as well as the momentum transfer $\vec{q}$. However, the recent work of Moriarity,[25] in which he uses refinements of this theory previously applied only to the noble metals, looks extremely promising. We strongly encourage such work, though complicated and tedious, because once a pseudopotential is derived it can be used for many properties in the future.

It is worth pointing out that in the screening of our pseudopotential (except for the empirical part taken from SF), band-structure effects were not included. These can be important at very long wavelengths, where the screening is done solely by electrons near the Fermi surface. The long-wavelength limit of the form factor is inversely proportional to the density of states at the Fermi energy, differing significantly from the free-electron value of $-\frac{2}{3}E_F$. It is not hard to convince oneself by looking at results of band-structure calculations that for $q \gtrsim 0.1k_F$ the free-electron picture should be a fairly good approximation. This is because electrons near Bragg planes are relatively fewer as q becomes larger, and the electrons that do the screening ($k \leq k_F$ and $|\vec{k}+\vec{q}| \geq k_F$) become much more numerous. Also, in the electron-phonon interaction the very-long-wavelength scattering is given very little weight except for effects at very low temperatures.

In our electron-phonon matrix element we nor-

malize the pseudo-wave-function instead of the true wave function. Correcting for this approximation would increase our resistivities and inverse lifetimes by about 5%.

By treating the trial distribution function as an expansion in spherical harmonics, we were able to investigate the importance of the distribution function at various temperatures. However, phonon drag effects which are significant at low temperatures are neglected in our calculation. According to the estimate of Lawrence and Wilkins,[38] the electron-electron effect is negligible above about 1 or 2°K. We find that the proper treatment of umklapp processes does not by itself cause significant deviations from the T^5 law. This is consistent with the theory of Lawrence and Wilkins.[39]

We find that the thermal resitivity was also quite sensitive to the directional anisotropy of the trial function, but not as much as was the case for the electrical resistivity.

The scattering times for ultrasonic attenuation were also calculated and found to be much more dependent upon crystal orientation than the electrical and thermal resistivities. It appears that the former are more sensitive to the Fermi surface.

We calculated quasiparticle lifetimes at the Fermi surface and found that the T^3 law was not obeyed. Though our calculation is very crude for temperatures in the region below 10°K, our results are consistent with cyclotron resonance and size-effect data.

ACKNOWLEDGMENTS

The author is deeply indebted to Prof. J. C. Swihart for suggesting this project and for his help and encouragement throughout. The author has also benefited from many enlightning discussions with Prof. J. P. Carbotte. This research was supported in part by NSF Grants DMR 73-07590 and DMR 77-10549, and in part by the National Research Council of Canada.

---

*Based in part on the Ph.D. thesis of the author, submitted to the Faculty of the Graduate School of Indiana University.

†Present address: Decision Science Application, Inc., 1401 Wilson Blvd., Arlington, Va.

[1]L. S. Sham, Proc. Phys. Soc. Lond. 78, 895 (1961).

[2]N. W. Ashcroft and J. W. Wilkins, Phys. Lett. 14, 285 (1965); J. C. Swihart, D. J. Scalapino, and Y. Wada, Phys. Rev. Lett. 14, 106 (1965).

[3]J. P. Carbotte and R. C. Dynes, Phys. Rev. 172, 476 (1968).

[4]P. B. Allen, M. L. Cohen, L. M. Falicov, and R. V. Kasowski, Phys. Rev. Lett. 21, 1794 (1969).

[5]P. B. Allen and M. L. Cohen, Phys. Rev. 187, 525 (1969).

[6]J. F. Balsley and J. C. Swihart, *Proceedings of the Twelfth International Conference on Low Temperature Physics*, edited by E. Kanda (Keigaka, Tokyo, 1971), p. 303; J. F. Balsley, Ph.D. thesis (Indiana University, 1969) (unpublished).

[7]P. T. Truant and J. P. Carbotte, Solid State Commun. 11, 443 (1972).

[8]P. Pecheur and G. Toussaint, Phys. Rev. B 7, 1223 (1973); J. Phys. Chem. Solids 33, 2281 (1972).

[9]R. W. Stark and L. M. Falicov, Phys. Rev. Lett. 19, 795 (1967).

[10]B. N. Aleksandrov and E. G. D'Yakov, Zh. Eksp. Teor. Fiz. 43, 852 (1962); Sov. Phys. JETP 16, 603 (1963)].

[11]K. Mendelssohn and H. M. Rosenberg, Proc. Phys. Soc. Lond. A 65, 385 (1952).

[12]P. G. Tomlinson and J. C. Swihart, Phys. Cond. Matter 19, 117 (1975); P. G. Tomlinson, Ph.D. thesis (Indiana University, 1973) (unpublished).

[13]L. Almqvist and R. Stedman, J. Phys. F 1, 785 (1971).

[14]P. G. Tomlinson and J. C. Swihart, preceding paper, Phys. Rev. B 19, 1867 (1979); referred to as I.

[15]P. G. Tomlinson and J. C. Swihart, in *Low Temperature Physics LT*-13, edited by K. D. Timmerhaus, W. J. O'Sullivan, and E. F. Hammel (Plenum, New York, 1974), Vol. 4, p. 1269.

[16]David Nowak, Phys. Rev. B 6, 3691 (1972).

[17]H. K. Leung, Ph.D. thesis (McMaster University, 1974) (unpublished).

[18]G. Gilat, G. Rizzi, and G. Cubiotti, Phys. Rev. 185, 971 (1969).

[19]N. Chesser and J. D. Axe, Phys. Rev. B 9, 4060 (1974).

[20]J. M. Ziman, *Electrons and Phonons* (Oxford U.P., London, 1960).

[21]Allen, Cohen, Falicov, and Kasowski (Ref. 5) report a value of 0.59 for this quantity, but a value of 0.54 is more consistent with their Fig. 1.

[22]R. W. Shaw, Jr., Phys. Rev. 174, 769 (1968).

[23]R. W. Shaw, Jr., J. Phys. C 2, 2350 (1969).

[24]M. Appapillai and A. R. Williams, J. Phys. F 3, 759 (1973).

[25]J. A. Moriarty, Phys. Rev. B 10, 3075 (1974).

[26]Y. Bergman, M. Kaveh, and N. Wiser, Phys. Rev. Lett. 32, 606 (1974).

[27]R. S. Sorbello, Solid State Commun. 12, 287 (1973).

[28]M. S. Steinberg, Phys. Rev. 109, 1486 (1958).

[29]A. B. Bhatia and R. A. Moore, Phys. Rev. 121, 1075 (1961).

[30]M. J. Lea, J. D. Llewellyn, D. R. Peck, and E. R. Dobbs, Proc. R. Soc. A 334, 357 (1973).

[31]V. F. Gantmakher, Zh. Eksp. Teor. Fiz. 43, 345 (1962) [Sov. Phys. JETP 17, 700 (1963)].

[32]M. Ya Azbel' and E. A. Kaner, Zh. Eksp. Teor. Fiz. 39, 80 (1960) [Sov. Phys. JETP 12, 58 (1961)].

[33]J. F. Koch and R. E. Doezema, Phys. Rev. Lett. 24, 507 (1970); R. E. Doezema and J. F. Koch, Phys. Rev. B 6, 207 (1972).

[34]P. B. Allen, *Proceedings of the Twelfth International Conference on Low Temperature Physics*, edited by E. Kanda (Kergaka, Tokyo, 1971), p. 517.

[35]D. M. Brookbanks, J. Phys. F 3, 988 (1973).
[36]A. Myers, R. S. Thompson, and Z. Ali, J. Phys. F 4, 1707 (1974).
[37]S. Auluck, J. Low Temp. Phys. 12, 601 (1973).
[38]W. F. Lawrence and J. W. Wilkins, Phys. Rev. B 7, 2317 (1973).
[39]W. F. Lawrence and J. W. Wilkins, Phys. Rev. B 6, 4466 (1972).
[40]R. L. Powell and W. A. Blanpied, U. S. Natl. Bur. Stand. Circ. No. 556, 1964 (unpublished).
[41]After this manuscript was completed, we became aware of the experimental work of J. E. A. Alderson and C. M. Hurd [Phys. Rev. B 12, 501 (1975)]. Their measured anisotropy of the electrical resistivity of zinc agrees with that of Ref. 10 as plotted in Fig. 5, but they fill in more detail near the maximum. Their maximum ratio of 1.36 agrees well with our previous calculation (Ref. 12) in which the pseudopotential used was SF (Ref. 9) extrapolated to Shaw's optimized model potential (Ref. 23) at small-q values. Our present calculation of Fig. 5, in which the pseudopotential was SF extrapolated to Appapillai and Williams (Ref. 24), gives a slightly lower anisotropy at the maximum. For both calculations the maximum occurs at 25 °K compared with the experimental maximum at 30 °K. We wish to thank Dr. Hurd for sending us a copy of their paper before publication.